2024 European Control Conference (ECC)
June 25-28, 2024. Stockholm, Sweden

LMI-based control design with robust local stability guarantees for linear discrete-time systems with input saturations

William D'Amico, Simone Zanini, Alessio La Bella, and Marcello Farina

***Abstract*— In this work we provide a data-based controller design method for uncertain input-saturated linear systems, where conditions based on linear matrix inequalities (LMIs) are exploited to guarantee robust global and regional closed-loop stability. The method is tested in simulation on a realistic case-study: the trade-off between performances and the region of validity of the established stability conditions is analysed.**

***Index Terms*— Linear matrix inequalities, virtual reference feedback tuning, regional stability.**

I. Introduction

Control design methods based on linear matrix inequalities (LMIs) have been extensively investigated [1]. They are particularly suited for providing optimality and robustness with respect to model uncertainties, as well as controllers appropriate for the decentralized/distributed framework [2]. Even model-free methods, e.g., virtual reference feedback tuning (VRFT) [3], lead to data-based LMI control design procedures [4]. All these methods, when applied to linear plants, are capable of guaranteeing closed-loop global asymptotic stability properties. However, in presence of nonlinearities such as input saturations, the latter cannot always be conferred, e.g., if the controlled system is unstable [5]. For this reason, LMI methods with regional validity have been proposed, particularly suited in case of static sector-bound nonlinearities, as the ones induced by saturations [6]. These methods have been also investigated for controllers with integrators and anti-windup actions, however without considering systems with uncertain parameters [5].

In this work we provide a data-based controller design method for uncertain input-saturated linear systems. Global and regional LMI-based stability conditions are provided, showing how the latter can be combined with two alternative control design strategies, namely $\mathcal{H}_2$ control and VRFT, both formulated as LMI problems.

Regarding $\mathcal{H}_2$ control, a wide literature is available, especially for the continuous-time case, e.g., [7]–[9] where in [7] and [8] model uncertainties are considered, whereas [9] accounts for actuator saturations.

An alternative approach, combining the VRFT algorithm discussed in [4] and a novel LMI-based formulation for disturbance rejection (named virtual disturbance feedback tuning, VDFT) is also proposed. The latter guarantees response speed and disturbance rejection capabilities at the same time.

The authors are with DEIB, Politecnico di Milano, Italy. Corresponding author: alessio.labella@polimi.it. This work has been financially supported by the PRIN 2022 project Control of Assistive Robots in crowded Environments (CARE, Id. 20225LX9M3), and by the Italian Ministry of Enterprises through the project 4D Drone Swarms (4DDS) under grant no. F/310097/01-04/X56.

A similar idea is discussed in [10], where the controller transfer function is identified with standard tools and closed-loop stability is not addressed.The proposed control methods are tested on a realistic simulation case-study. A detailed analysis of the trade-off between the achieved performances and the corresponding region of validity is carried out.

A. Notation

The symmetric matrix $\begin{bmatrix} A & B^\top \\ B & C \end{bmatrix}$ is abbreviated as $\begin{bmatrix} A & \star \\ B & C \end{bmatrix}$. $0_{n,m}$ (or 0) denotes a zero matrix with n rows and m columns (or with a suitable number of rows and columns), whereas I_n (or I) is the identity matrix of dimension n (or with suitable dimensions). $|a|$ is the absolute value of a real number a, $\|v\| = \sqrt{v^\top v}$ denotes the 2-norm of a vector v. Also, k denotes the discrete-time index and q the forward shift operator (i.e., $u(k+1) = qu(k)$, for a signal $u(k)$). Given a signal $u(k)$, the variable $u_F(k)$ indicates the signal obtained by filtering $u(k)$ through a transfer function $F(q)$, i.e., $u_F(k) = F(q)u(k)$ (when applied to a vector, $F(q)$ is intended element-wise). Finally, $\|F(q)\|_{\mathcal{H}_2} = \sqrt{\frac{1}{2\pi}\int_{-\pi}^{\pi} |F(e^{j\omega})|^2 \, d\omega}$ denotes the $\mathcal{H}_2$-norm of $F(q)$.

II. Problem statement

A. The system and the uncertain model

Consider the following discrete-time system $\mathcal{S}$ of order n

$$\mathcal{S} \; : \; \begin{cases} z(k+1) = \theta^{o\top}\phi(k) + \delta(k) \\ y_m(k) = z(k) + w(k) \end{cases}, \tag{1}$$

where $\phi \in \mathbb{R}^{2n}$ is the regressor vector, defined as

$$\phi(k) = [z(k), ..., z(k-n+1), u(k), ..., u(k-n+1)]^\top, \tag{2}$$

$u \in \mathbb{R}$ is the system input, $z \in \mathbb{R}$ is the noise-free output, $\delta \in \mathbb{R}$ is the process disturbance, $w \in \mathbb{R}$ is the measurement noise, $y_m \in \mathbb{R}$ is the measured output, and $\theta^o = \left[\theta_1^o, ..., \theta_{2n}^o\right]^\top \in \mathbb{R}^{2n}$ is the vector of unknown system parameters. The following assumption is stated.

Assumption 1: The system (1) is asymptotically stable and its order n is known. Also, w in (1) is bounded and its upper bound is known, i.e., there exists a known $\bar{w} > 0$ such that $|w(k)| \leq \bar{w}$ for all $k \geq -n+1$. Moreover, δ in (1) is bounded, i.e., $\exists\, \bar{\delta} > 0$, possibly not known, such that $|\delta(k)| \leq \bar{\delta}$ for all $k \geq 0$. □

Given the previous assumption, following the same lines of [4], the system (1) can be described by the uncertain model

$$\begin{cases} x(k+1) = A(\theta)x(k) + B(\theta)u(k) + B_\xi \xi(k) \\ y_m(k) = Cx(k) \end{cases}, \tag{3}$$

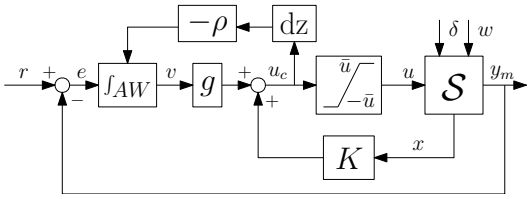

Fig. 1: Control scheme with symmetric saturation, explicit integral action with anti-windup, and static state feedback.

where the measurable state $x(k) \in \mathbb{R}^{2n-1}$ is

$$x(k) = [y_m(k), ..., y_m(k-n+1), u(k-1), ..., u(k-n+1)]^\top, \quad (4)$$

whereas $\xi(k)$, acting as a bounded exogenous disturbance, derives from the effect of $\delta(k)$ and $w(k)$ on the state evolution. The system matrices have the following form, consistent with the state definition:

$$A(\theta) = \begin{bmatrix} \theta_1 & \dots & \theta_n & \theta_{n+2} & \dots & \theta_{2n} \\ I_{n-1} & & 0_{n-1,1} & & 0_{n-1,n-1} & \\ & 0_{1,n} & & & 0_{1,n-1} & \\ & 0_{n-2,n} & & & I_{n-2} & 0_{n-2,1} \end{bmatrix},$$

$B(\theta) = \begin{bmatrix} \theta_{n+1} & 0_{1,n-1} & 1 & 0_{1,n-2} \end{bmatrix}^\top$, $B_\xi^\top = C = \begin{bmatrix} 1 & 0_{1,2n-2} \end{bmatrix}$.

The vector $\theta \in \Theta$ identifies the uncertain model parameters, where Θ is a convex and compact polytope with known vertices θ^{V_i}, $i = 1, \dots, n_v$, possibly defined by using collected input/output data (cf. [4]). In view of this, although $A(\theta)$ and $B(\theta)$ are uncertain, they can be defined as

$$\begin{bmatrix} A(\theta) & B(\theta) \end{bmatrix} = \sum_{i=1}^{n_v} \beta_i \begin{bmatrix} A(\theta^{V_i}) & B(\theta^{V_i}) \end{bmatrix}, \quad (5)$$

where $A(\theta^{V_i})$ and $B(\theta^{V_i})$ are defined as reported above, whereas $\beta_1 \geq 0, \dots, \beta_{n_v} \geq 0$ are unknown scalars, defined such that $\sum_{i=1}^{n_v} \beta_i = 1$.

B. The control scheme

Consider the control scheme in Figure 1 where r is the reference. The control input u_c is limited by a symmetric saturation with known level $\bar{u} > 0$, i.e.,

$$u(k) = \mathrm{sat}(u_c(k)) = \begin{cases} \bar{u} & \text{if } u_c(k) > \bar{u} \\ u_c(k) & \text{if } -\bar{u} \leq u_c(k) \leq \bar{u} \\ -\bar{u} & \text{if } u_c(k) < -\bar{u} \end{cases}. \quad (6)$$

The block "$\int AW$" denotes a anti-windup integrator, with equation $v(k) = v(k-1) + e(k-1) - \rho\, \mathrm{dz}(u_c(k-1))$, where $\mathrm{dz}(u_c(k)) = u_c(k) - \mathrm{sat}(u_c(k))$ is the deadzone function, and $u_c(k) = Kx(k) + gv(k)$. Note that, in the integrator expression, the term $-\rho\, \mathrm{dz}(u_c(k-1))$ is introduced to provide an anti-windup action, contrasting the integrator windup when $\mathrm{dz}(u_c) \neq 0$, i.e., when the input saturates. The tuning parameters are the static state-feedback gain K, the static integrator gain g, and the anti-windup static gain ρ. The objective of this work is to design a controller which allows us to provide robust exponential stability guarantees and, at the same time, suitable performances.

III. Control design

A. Robust stability guarantees

By considering (3) and the control scheme depicted in Figure 1, the closed-loop system equations read as

$$\begin{cases} \chi(k+1) = A_\chi(\theta)\chi(k) + B_\chi(\theta)\, \mathrm{dz}(J\chi(k)) + \eta(k) \\ y_m(k) = C_\chi \chi(k) \end{cases}, \quad (7)$$

where $\chi(k) = \begin{bmatrix} x(k) \\ v(k) \end{bmatrix}$, $A_\chi(\theta) = \widetilde{A}(\theta) + \widetilde{B}(\theta)J$, $\widetilde{A}(\theta) = \begin{bmatrix} A(\theta) & 0 \\ -C & 1 \end{bmatrix}$, $\widetilde{B}(\theta) = \begin{bmatrix} B(\theta) \\ 0 \end{bmatrix}$, $J = \begin{bmatrix} K & g \end{bmatrix}$, $B_\chi(\theta) = \widetilde{D}(\theta) + \widetilde{E}\rho$, $\widetilde{D}(\theta) = \begin{bmatrix} -B(\theta) \\ 0 \end{bmatrix}$, $\widetilde{E} = \begin{bmatrix} 0 \\ -1 \end{bmatrix}$, $C_\chi = \begin{bmatrix} C & 0 \end{bmatrix}$, and $\eta(k) = \begin{bmatrix} B_\xi \xi(k) \\ r(k) \end{bmatrix}$. The following result provides conditions for the local and global robust exponential stability of the origin, i.e., $(\bar{\eta}, \bar{\chi}, \bar{y}_m) = (0, 0, 0)$, for all the models (7) with θ lying in the uncertainty set Θ.

Proposition 3.1: Assume that $r = w = \delta = 0$. The origin is a locally exponentially stable equilibrium for system (7) for all $\theta \in \Theta$, where $\mathcal{E}(Q) = \{\chi \in \mathbb{R}^{2n} : \chi^\top Q^{-1} \chi \leq 1\}$ is a forward invariant set contained in the basin of attraction of the origin, if there exist $Q = Q^\top \in \mathbb{R}^{2n \times 2n}$, $L \in \mathbb{R}^{1 \times 2n}$, $Y \in \mathbb{R}^{1 \times 2n}$, $\tau \in \mathbb{R}$, $\mu \in \mathbb{R}$ such that

$$\begin{bmatrix} Q & \star & \star \\ -L - Y & 2\tau & \star \\ \widetilde{A}(\theta^{V_i})Q + \widetilde{B}(\theta^{V_i})L & \widetilde{D}(\theta^{V_i})\tau + \widetilde{E}\mu & Q \end{bmatrix} \succ 0 \quad (8)$$

for all $i = 1, \dots, n_v$, and

$$\begin{bmatrix} Q & Y^\top \\ Y & \bar{u}^2 \end{bmatrix} \succeq 0\,. \quad (9)$$

Moreover, the origin is a globally exponentially stable equilibrium for (7) for all $\theta \in \Theta$, if (8) holds with $Y = 0$ and for all $i = 1, \dots, n_v$. In both cases, the stabilizing control gains are given by $\begin{bmatrix} K & g \end{bmatrix} = LQ^{-1}$, $\rho = \mu\tau^{-1}$. □

The proof of this proposition follows straightforwardly from [5], with the difference that the proposed conditions hold robustly on a set of possible models in view of (5).

B. Performances

In this section, two alternative design approaches are discussed, where the previous stability constraints can be naturally included. The first method relies on a novel reformulation of the VRFT problem for disturbance rejection, as initially proposed in [10]. The second one is based on the $\mathcal{H}_2$ control formulation adopted in [11]. While stability properties are guaranteed by Proposition 3.1 in a defined region $\mathcal{E}(Q)$ even in presence of input saturations, performances are guaranteed under the following assumption.

Assumption 2: The input is not saturated, i.e., $u_c = u$. □

Two important remarks are due. First, while stability guarantees are provided by Proposition 3.1 under the assumption that $\delta = r = 0$, the performances are enforced possibly for any reference r and disturbance δ; this is, from the theoretical standpoint, in contradiction with the assumptions of Proposition 3.1. However, the stability result in Proposition 3.1 still holds, e.g., also when piecewise-constant reference and

disturbance variations are such that the current state lies in a positively invariant set centred in the new steady state (defined based on the non-zero output reference and disturbance) and verifying the sector condition imposed by the input saturation (see [5]) or when disturbances are impulsive and are accounted to as state perturbations driving state jumps, as long as $x(k) \in \mathcal{E}(Q)$. A more comprehensive extension to non-zero disturbances and references will be subject of future work. Secondly note, from Figure 1, that when Assumption 2 holds $\mathrm{dz}(u_c) = 0$, meaning that parameter ρ does not influence the dynamics of the control system. For this reason, ρ (or, more specifically, μ and τ) is not used as optimization variable in purely performance-oriented LMI problems, but only in the stability one.

1) VRFT/VDFT combined approach: Considering system (1) and the separation principle, we can denote with $y(k)$ and $d(k)$ the components of $z(k)$ depending upon $u(k)$ and $\delta(k)$, respectively, i.e.,

$$y(k+1) = \theta^{o\top} \hat{\phi}(k)\,, \tag{10a}$$

$$d(k+1) = \theta_\zeta^{o\top} \zeta(k) + \delta(k) \tag{10b}$$

where $\hat{\phi}(k) = [y(k), ..., y(k-n+1), u(k), ..., u(k-n+1)]^\top$, $\zeta(k) = [d(k), ..., d(k-n+1)]^\top$, and $\theta_\zeta^{o\top} = [\theta_1^o, ..., \theta_n^o]^\top$. Note that $z(k) = y(k) + d(k)$ and that $y_m(k) = y(k) + d(k) + w(k)$. With reference to (10) and Figure 1, to enforce a predefined closed-loop response speed, in [4] a VRFT-based method was proposed to design the control gains that allow the transfer function between the reference r and the output variable y_m (denoted $M_{K,g}(q)$) to be as close as possible to a reference one (denoted $M(q)$). In this section a similar but alternative novel LMI-based formulation (named virtual disturbance feedback tuning, VDFT) is proposed for disturbance rejection, where the control gains are identified such that the sensitivity function $S_{K,g}(q)$ (i.e., the one between disturbance d and y_m in closed loop) is as similar as possible to a given reference one $S(q)$, i.e., it is a solution to

$$\underset{K,g}{\text{minimize}}\ J_{MR}(K,g) \coloneqq \|(S(q) - S_{K,g}(q))W(q)\|_{\mathcal{H}_2}^2, \tag{11}$$

where $W(q)$ is a suitable weighting function. To do so, we need two datasets of input and output data collected with the same inputs $u_c(k) = u(k)$ but with different noise realizations, i.e., $(u(k), y_m^1(k))$ and $(u(k), y_m^2(k))$, for $k = -n+1, \ldots, N$, under the next assumption.

Assumption 3: a) The output signals $y_m^1(k)$ and $y_m^2(k)$ are collected in absence of process disturbance, i.e., $\delta(k) = 0$, for all $k = -n+1, \ldots, N$, implying that $y_m^i(k) = y(k) + w^i(k)$, $i = 1, 2$.
b) The signals $u(k)$, $w^1(k)$, and $w^2(k)$ are uncorrelated, with $w^1(k)$ and $w^2(k)$ being stationary zero-mean processes. □

Note that, to fulfill Assumption 3*a)*, data may be collected in a test environment, e.g., in a laboratory, where the process disturbance can be absent, or, if it is not possible, by simulating an identified model, where the noise w can be generated from an estimated probability distribution (cf. [4]).

As done in [10], a *virtual disturbance* signal $\tilde{d}^i$ is introduced for the two collected datasets, and, consequently, a *virtual measured output* signal $\tilde{y}_m^i$, is defined as

$$\tilde{y}_m^i(k) = y(k) + w^i(k) + \tilde{d}^i(k) = y_m^i(k) + \tilde{d}^i(k) = S(q)\tilde{d}^i(k),$$

for $i = 1, 2$. It follows that the *virtual disturbance* and the *virtual measured output* can be computed from the collected output data for each i-th experiment as

$$\tilde{d}^i(k) = \frac{y_m^i(k)}{S(q) - 1}, \quad \tilde{y}_m^i(k) = \frac{S(q)\, y_m^i(k)}{S(q) - 1}\,. \tag{12}$$

Let $r = 0$ in Figure 1, the following steps are carried out to obtain a VDFT-based cost function for each collected experiment, i.e., $i = 1, 2$,

1) Compute the *virtual measured output* sequences $\tilde{y}_m^i(k)$ according to (12).
2) Compute the *virtual error* sequences $\tilde{e}^i(k) = -\tilde{y}_m^i(k)$.
3) Compute the *integrated virtual error* sequences according to the recursive equation $\tilde{v}^i(k) = \tilde{v}^i(k-1) + \tilde{e}^i(k-1)$, with initial condition $\tilde{v}^i(-n+1) = 0$.
4) Compute *virtual state* sequences $\tilde{x}^i(k)$ according to (4) by using $\tilde{y}_m^i$ in place of y_m.
5) Compute the filtered sequences $\tilde{x}_F^i(k) = F(q)\tilde{x}^i(k)$, $u_F(k) = F(q)u(k)$, $\tilde{v}_F^i(k) = F(q)\tilde{v}^i(k)$, where the filter $F(q)$ will be defined later.
6) Define $\mathbf{u} \coloneqq \begin{bmatrix} u_F(0) & \ldots & u_F(N-1) \end{bmatrix}^\top$ and

$$X^i \coloneqq \begin{bmatrix} \tilde{x}_F^i(0)^\top & \tilde{v}_F^i(0) \\ \vdots & \vdots \\ \tilde{x}_F^i(N-1)^\top & \tilde{v}_F^i(N-1) \end{bmatrix},$$

$$\mathbf{u}_N \coloneqq \frac{1}{2N}\left((X^1 + X^2)^\top \mathbf{u}\right), \tag{13}$$

$$\mathbf{X}_N \coloneqq \frac{1}{2N}\left((X^1)^\top X^2 + (X^2)^\top X^1\right). \tag{14}$$

We require the following assumption, verified under structural identifiability conditions and persistency of excitation.

Assumption 4: $\mathbf{X}_N \succ 0$. □

To minimize (11), in such a way that the stability conditions can be also included in the optimization problem, we rely on the following result.

Theorem 3.2: Let Assumptions 1, 2, 3, and 4 hold. The following optimization problem is, for $N \to +\infty$,

$$\underset{L,\sigma}{\text{minimize}}\ \ \sigma \tag{15a}$$

$$\text{subject to} \begin{bmatrix} \sigma + 2L\mathbf{X}_N^{-1}\mathbf{u}_N - \mathbf{u}_N^\top \mathbf{X}_N^{-1} Q \mathbf{X}_N^{-1}\mathbf{u}_N & L \\ L^\top & Q \end{bmatrix} \succcurlyeq 0\,, \tag{15b}$$

equivalent to (11) if, for any $\gamma_{\mathrm{x}} > 0$, it holds that

$$|F(e^{j\omega})|^2 = \frac{|S_{K,g}(e^{j\omega})|^2 |S(e^{j\omega}) - 1|^2 |W(e^{j\omega})|^2}{|1 - C_K(e^{j\omega})|^2 \Phi_u(\omega)}\,, \tag{16}$$

$$Q = \gamma_{\mathrm{x}} \mathbf{X}_N\,, \tag{17}$$

where Φ_u is the spectral density of u, whereas

$$C_K(q) = k_{n+1} q^{-1} + \cdots + k_{2n-1} q^{-n+1}\,, \tag{18}$$

and

$$\begin{bmatrix} K & g \end{bmatrix} = LQ^{-1}\,. \tag{19}$$

Moreover, for $N \to +\infty$, under (16), (19), and for any $Q = Q^\top \succ 0$, the optimization problems (15) and (11) have the same minimum point, i.e., $\begin{bmatrix} K & g \end{bmatrix} = \mathbf{u}_N^\top \mathbf{X}_N^{-1}$. □

Proof: See the Appendix. ■

The filter $F(q)$ in (16) cannot be defined since it depends on the system and controller transfer functions. Therefore, the following approximation is proposed:

$$F(q) = S(q)(S(q)-1)W(q)/U(q)\,, \tag{20}$$

where $U(q)$ is such that $|U(e^{j\omega})|^2 = \Phi_u(\omega)$, which may be known or estimated from input data (cf. [12]). A possible way to achieve a more accurate approximation of the filter (16) is to preliminarily solve (15) using (20), and then to use the obtained parameters K to get an estimate of $1 - C_K(q)$ to be included in (20) before solving (15) for a second time. Finally, condition (17) can be either neglected or relaxed by defining the matrix Q and the scalar γ_{x} as free optimization variables, replacing (17) with a couple of constraints (cf. [4, Eq. (34)]). Importantly, the VRFT and VDFT approaches can also be combined together. Indeed, given two datasets $(u(k), y^1(k))$ and $(u(k), y^2(k))$, for $k = -n+1, \dots, N$, collected from the open-loop system under Assumption 3, the overall algorithm with robust local stability guarantees consists of the following steps.

1) Solve the LMI optimization problem

$$\underset{L, Y, Q=Q^\top, \sigma, \sigma_r, \tau, \mu}{\text{minimize}} \quad c_d\sigma + c_r\sigma_r \tag{21}$$

subject to (8) for $i = 1, \dots, n_v$, (9), (15b), [4, Eq. (29)] [1], where c_d and c_r are user-defined weights.
2) If feasible, set $\begin{bmatrix} K & g \end{bmatrix} = LQ^{-1}$, and $\rho = \mu\tau^{-1}$.
3) Replace $L = \begin{bmatrix} K & g \end{bmatrix} Q$ and $\mu = \rho\tau$ in (8), since $\begin{bmatrix} K & g \end{bmatrix}$ and ρ are now known, and, to obtain the maximum guaranteed region of attraction $\mathcal{E}(Q)$, solve the LMI problem

$$\begin{aligned} &\underset{Y, Q=Q^\top, \tau, \gamma_q}{\text{maximize}} \quad \gamma_q \\ &\text{subject to (8) for } i = 1, \dots, n_v,\ (9),\ Q \succeq \gamma_q I\,. \end{aligned} \tag{22}$$

Note that, given the inclusion of (8) and (9) in the optimization problem (21), the procedure ensures not only desired performances, but also robust local exponential stability of the origin. Note that, in (21) and later in (27), global exponential stability guarantees can be achieved by neglecting (9) and by setting $Y = 0$ in (8), for $i = 1, \dots, n_v$.

$\mathcal{H}_2$ regulation

In this section we derive a cost function based on the $\mathcal{H}_2$ formulation considered in [11]. Under Assumption 2, the state equation of the feedback system (7) reduces to

$$\chi(k+1) = (\widetilde{A}(\theta) + \widetilde{B}(\theta)J)\chi(k) + \eta(k)\,, \tag{23}$$

[1] In [4, Eq. (29)] σ_r is place of σ and Q in place of G. Also, since the integrator is here strictly proper, differently from the one in [4], the result in [4, Th. 2] still holds with the difference that $E = I$ and $D(q) = q - 1$. The filter in [4, Eq. (23)] can still be used as approximation.

where $u(k) = J\chi(k)$ and $J = \begin{bmatrix} K & g \end{bmatrix}$. We consider the performance output $y^*(k)$ defined as

$$y^*(k) := C^*\chi(k) + D^*u(k) = (C^* + D^*J)\chi(k) \tag{24}$$

where C^*, D^* are fixed user-defined matrices. The transfer matrix from the exogenous input η to y^* is denoted by $G^*_{K,g,\theta}(q) := (C^* + D^*J)(qI - (\widetilde{A}(\theta) + \widetilde{B}(\theta)J))^{-1}$. Our objective is to minimize the maximal $\mathcal{H}_2$-norm $\|G^*_{K,g,\theta}(q)\|_{\mathcal{H}_2}$ for any possible model parameterization, i.e., to solve

$$\underset{K, g, \gamma}{\text{minimize}} \quad \gamma \tag{25a}$$

$$\text{subject to} \quad \|G^*_{K,g,\theta}(q)\|_{\mathcal{H}_2} < \gamma \quad \text{for all } \theta \in \Theta\,. \tag{25b}$$

The following result shows that the previous problem can be reformulated as an LMI problem.

Proposition 3.3: Let Assumptions 1 and 2 hold. The optimization problem (25) is equivalent to

$$\underset{L, Q=Q^\top, Z=Z^\top, \widetilde{\gamma}}{\text{minimize}} \quad \widetilde{\gamma} \tag{26a}$$

$$\text{subject to} \quad \begin{bmatrix} Z & I \\ I & Q \end{bmatrix} \succeq 0\,,\ \operatorname{tr}(Z) < \widetilde{\gamma}\,, \tag{26b}$$

$$\begin{bmatrix} Q & \star & \star \\ \widetilde{A}(\theta^{V_i})Q + \widetilde{B}(\theta^{V_i})L & Q & \star \\ C^*Q + D^*L & 0 & I \end{bmatrix} \succ 0 \text{ for } i = 1, \dots, n_v, \tag{26c}$$

where $\gamma = \sqrt{\widetilde{\gamma}}$ and $\begin{bmatrix} K & g \end{bmatrix} = LQ^{-1}$. □

Proof: See the Appendix. ■

The overall control design algorithm with robust local stability guarantees consists of the following.

1) Solve

$$\underset{L, Y, Q=Q^\top, Z=Z^\top, \widetilde{\gamma}, \tau, \mu}{\text{minimize}} \quad \widetilde{\gamma} \tag{27}$$

subject to (8) and (26c) for $i = 1, \dots, n_v$, (9), (26b).
Then, Steps 2) and 3) reported after (21) are also applied.

IV. Simulation results

The algorithms are tested on a simulation example derived from [13]. More details on the benchmark parameters are available in [14, Chapter 4]. The case study is a water tank heated by a thermal plate, with ingoing and outgoing water flows. The system is discretized using a sample time $T_s = 100$ s, and is rewritten in form (1), where $n = 2$, $\theta^o = \begin{bmatrix} 1.3306 & -0.3698 & 1.0481 & 0.7536 \end{bmatrix}^\top$ and $\delta(k) = 0.06717 d_{T_i}(k) - 0.02795 d_{T_i}(k-1)$. Two datasets composed of $N = 1000$ samples are collected using a PRBS in $[-1, 1]$ as input u (i.e., the thermal power).The set Θ, resulting from set membership identification [4], has 30 vertices. Regarding VRFT/VDFT, we use $M(q) = \frac{(1-a)q^{-1}}{q(1-aq^{-1})}$ and $S(q) = 1 - M(q)$ where a spans from 0.2 to 0.79 to analyse the sensitivity with respect to the convergence speed of the reference models. We also select $W(q) = 1$. In (21), we set $c_d = c_r = 1$. In Table I, for different values of the spectral radius a of the reference model, we display the spectral radii ρ^L_{CL} and ρ^G_{CL} of the closed-loop system state matrix $A_\chi(\theta^o)$ in (7) in case either the local or the global

TABLE I: VRFT/VDFT performances

a	0.2	0.38	0.5	0.6	0.7	0.74	0.79
ρ^L_{CL}	0.42	0.42	0.49	0.62	0.71	0.75	0.8
ρ^G_{CL}	0.42	0.42	0.49	0.62	0.71	0.75	0.8

TABLE II: $\mathcal{H}_2$ performances

$100c^*$	1	3	5	7	9	11	13	15
ρ^L_{CL}	0.58	0.53	0.48	0.44	0.42	0.39	0.37	0.36
ρ^G_{CL}	0.62	0.61	0.61	0.61	0.61	0.61	0.61	0.61

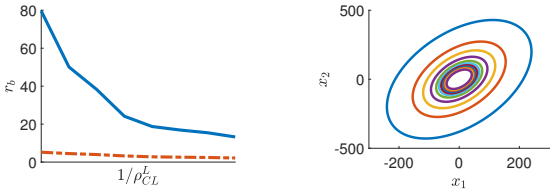

(a) (b)

Fig. 2: (a) Trade-off between performance and size of $\mathcal{E}(Q)$ for $\mathcal{H}_2$ (with $c^* \geq 0.05$). (b) Projections of $\mathcal{E}(Q)$ onto $\mathbb{R}^2$ for $\mathcal{H}_2$ with $c^* = 0.05, 0.06, \ldots, 0.15$.

condition in Proposition 3.1 is used, respectively. However, for the considered case study and the considered control configuration, we observe that with VRFT/VDFT both the stability conditions are always feasible and provide the same value of spectral radius. Also, in case the local condition is used, the sets $\mathcal{E}(Q)$ are numerically unbounded, witnessing the fact that the obtained controllers have a global validity.

A different behaviour is obtained regarding $\mathcal{H}_2$. For its application, we define

$$C^* = \begin{bmatrix} c^* & 0 & 0 & 0 \\ 0 & 0 & 0 & c^* \\ 0 & 0 & 0 & 0 \end{bmatrix}, \quad D^* = \begin{bmatrix} 0 \\ 0 \\ d^* \end{bmatrix},$$

where $d^* = 0.01$, whereas c^* spans from 0.01 to 0.15. In Table II we show how the spectral radii ρ^L_{CL} and ρ^G_{CL} vary with c^* by considering the local and global conditions, respectively, which are both always feasible. However, even when increasing c^*, the global condition does not allow for improvements in the convergence speed of the closed-loop system, differently from the local condition. In Figure 2(a), the comparison between $1/\rho^L_{CL}$ and the radius r_b of the maximum hypersphere in $\mathcal{E}(Q)$ is shown, displaying a significant trade-off. Note also that, in Figure 2(a), the radius of the maximum hypersphere in $\mathcal{E}(Q)$ is computed based both on the matrix Q obtained in the design phase by solving (27) (red dashed line) and on the matrix Q calculated in a subsequent analysis phase by solving (22), i.e., after the control gains are available (blue solid line). In the latter case, the size of $\mathcal{E}(Q)$ is significantly larger than in the former case. The projections of $\mathcal{E}(Q)$, obtained by solving (22), onto $\mathbb{R}^2$ are displayed in Figure 2(b) in case $c^* = 0.05, 0.06, \ldots, 0.15$, where the states related to the output are depicted, i.e., $x_1(k) = y(k)$ and $x_2(k) = y(k-1)$. In the case study considered here, $\mathcal{H}_2$ allows us to obtain better performances, at the price of reducing the dimension of the guaranteed domain of attractions. This may be due

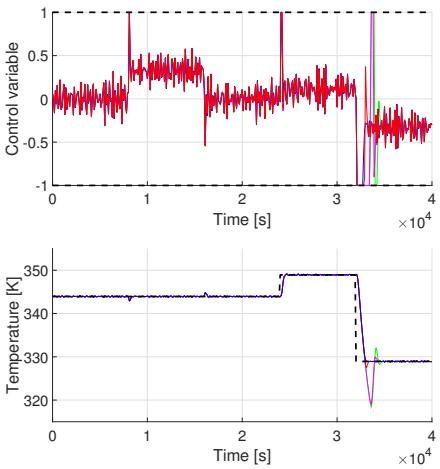

Fig. 3: Top panel: input trajectories. Bottom panel: output trajectories. Red lines: $\mathcal{H}_2$; green lines: $\mathcal{H}_2$ without anti-windup ($\rho = 0$); blue lines: VRFT/VDFT; magenta lines: VRFT/VDFT without anti-windup ($\rho = 0$). Black dashed lines: saturation limits (top panel), reference (bottom panel).

to different reasons. On the one hand, the reduction of the dimension of the guaranteed region of attraction may be due to the fact we are enforcing high performances robustly over a polytopic uncertainty set, differently from VRFT/VDFT, whose cost function is model-free. On the other hand, the reduced domain of attraction and lower spectral radii of $\mathcal{H}_2$ may be also due to the fact that $\mathcal{H}_2$ allows one to enhance the performances even beyond the zone of linear regime, differently from VRFT/VDFT, where the performances are strongly related to the region in which the data are collected. For a final comparison, in Figure 3 we show the simulation plots obtained by testing the controllers designed with VRFT/VDFT, with $a = 0.2$, and $\mathcal{H}_2$, with $c^* = 0.15$. The reference output varies as shown in the bottom panel of Figure 3, while a piecewise constant disturbance is applied, i.e., taking nonzero value $d_{T_i} = -15$ K only from $t = 8000$ s to $t = 16000$ s. The control input u is shown in the top panel of Figure 3. The simulations show that both the methods display similar results, but VRFT/VDFT provides better performances, in particular when the input saturates.

V. Conclusions

In this paper we propose suitable LMI problems to design a regulator enforcing regional robust stability properties and prescribed performances to a control system when the plant is affected by uncertainties and input saturations. Performances are enforced with two alternative control design strategies, i.e., $\mathcal{H}_2$ control and VRFT/VDFT. Future work will be devoted to the extension to plants described by neural networks.

Appendix

Proof of Theorem 3.2. First we show that minimizing (15) is equivalent to minimize the following function under (17)

$$\begin{aligned} J^N_{VR}(K,g) &= \frac{1}{N}(\mathbf{u} - X^1 \begin{bmatrix} K & g \end{bmatrix}^\top)^\top (\mathbf{u} - X^2 \begin{bmatrix} K & g \end{bmatrix}^\top) \\ &= \text{cst} + \begin{bmatrix} K & g \end{bmatrix} \mathbf{X}_N \begin{bmatrix} K & g \end{bmatrix}^\top - 2 \begin{bmatrix} K & g \end{bmatrix} \mathbf{u}_N , \end{aligned} \tag{28}$$

where cst $= \frac{1}{N}\mathbf{u}^\top\mathbf{u}$ is constant with respect to the optimization variables K and g, whereas $\mathbf{X}_N$ and $\mathbf{u}_N$ can be defined under Assumption 1. Under Assumption 4, $J^N_{VR}(K,g)$ has a global minimum in $\begin{bmatrix}K & g\end{bmatrix} = \mathbf{u}_N^\top\mathbf{X}_N^{-1}$. Now, let us consider

$$\widetilde{J}^N_{VR}(K,g) = (\begin{bmatrix}K & g\end{bmatrix}^\top - \mathbf{X}_N^{-1}\mathbf{u}_N)^\top Q(\begin{bmatrix}K & g\end{bmatrix}^\top - \mathbf{X}_N^{-1}\mathbf{u}_N).$$

By assumption, $Q = Q^\top \succ 0$, so the previous cost function $\widetilde{J}^N_{VR}(K,g)$ has a global minimum in $\begin{bmatrix}K & g\end{bmatrix} = \mathbf{u}_N^\top\mathbf{X}_N^{-1}$. Moreover, if we set Q as in (17), under Assumption 4, then minimizing $J^N_{VR}(K,g)$ is equivalent to minimize $\widetilde{J}^N_{VR}(K,g)$ since the two cost functions differ only for constant additive and strictly positive scaling terms. By defining $\begin{bmatrix}K & g\end{bmatrix}$ according to (19), then minimizing $\widetilde{J}^N_{VR}(K,g)$ is equivalent to minimizing, in the free variable L, $\widetilde{J}^N_{VR}(L) = (Q^{-1}L^\top - \mathbf{X}_N^{-1}\mathbf{u}_N)^\top Q(Q^{-1}L^\top - \mathbf{X}_N^{-1}\mathbf{u}_N) = LQ^{-1}L^\top - 2L\mathbf{X}_N^{-1}\mathbf{u}_N + \mathbf{u}_N^\top\mathbf{X}_N^{-1}Q\mathbf{X}_N^{-1}\mathbf{u}_N$, which is equivalent to

$$\begin{aligned}&\underset{L,\sigma}{\text{minimize}} \;\; \sigma \qquad (29)\\ &\text{subject to } \sigma \geq LQ^{-1}L^\top - 2L\mathbf{X}_N^{-1}\mathbf{u}_N + \mathbf{u}_N^\top\mathbf{X}_N^{-1}Q\mathbf{X}_N^{-1}\mathbf{u}_N.\end{aligned}$$

By resorting to the Schur complement, (29) can be recast as (15). Note that also if $Q = Q^\top \succ 0$ is a free variable, then the optimization problem (15) has global minima for $\sigma = 0$, which implies $LQ^{-1} = \begin{bmatrix}K & g\end{bmatrix} = \mathbf{u}_N^\top\mathbf{X}_N^{-1}$.

As a second step we show that, under the setting (16) and for $N \to +\infty$, minimizing the cost function $J^N_{VR}(K,g)$ in (28) is equivalent to minimizing $J_{MR}(K,g)$ in (11). Note that $J^N_{VR}(K,g) = \frac{1}{N}\sum_{k=0}^{N-1}\big(F(q)(u(k)-u^1_{K,g}(k))\big)\big(F(q)(u(k)-u^2_{K,g}(k))\big)$, where $u^i_{K,g}(k) = \begin{bmatrix}K & g\end{bmatrix}\begin{bmatrix}\tilde{x}^i(k)\\ \tilde{v}^i(k)\end{bmatrix} = B_K(q)\tilde{y}^i_m(k) + C_K(q)u(k) - gI(q)\tilde{y}^i_m(k)$, $B_K(q) = k_1 + k_2q^{-1} + ... + k_nq^{-n+1}$, $C_K(q)$ as in (18), and $I(q) = (q-1)^{-1}$. As discussed in [3], if $N \to +\infty$, $J^N_{VR}(K,g) \to \bar{J}_{VR}(K,g)$,

$$\begin{aligned}\bar{J}_{VR}(K,g) = \mathbb{E}[&\big(F(q)(u(k)-u^1_{K,g}(k))\big)\\ &\big(F(q)(u(k)-u^2_{K,g}(k))\big)]. \qquad (30)\end{aligned}$$

Also, $y(k) = G(q)u(k)$, where $G(q)$ is the unknown transfer function between u and y in (10a). Recalling (12) and Assumption 3*a)*, we also have that $\tilde{y}^i_m(k) = \frac{S(q)}{S(q)-1}(G(q)u(k) + w^i(k))$, and we can write $\bar{J}_{VR}(K,g) = \mathbb{E}[\big(F(q)D_{K,g}(q)u(k) + F(q)E_{K,g}(q)w^1(k)\big)\big(F(q)D_{K,g}(q)u(k) + F(q)E_{K,g}(q)w^2(k)\big)]$, where $D_{K,g}(q) = 1 - C_K(q) - S(q)(S(q)-1)^{-1}(B_K(q) - gI(q))G(q)$ and $E_{K,g}(q) = -S(q)(S(q)-1)^{-1}(B_K(q) - gI(q))$. In view of Assumption 3*b)*, we can write that $\bar{J}_{VR}(K,g) = \mathbb{E}\left[\left(F(q)D_{K,g}(q)u(k)\right)^2\right]$. According to Figure 1, under Assumption 2, we can compute $S_{K,g}(q)$, i.e., the real closed-loop transfer function between d and y_m: $S_{K,g}(q) = \frac{1}{1-R_{K,g}(q)}$, where $R_{K,g}(q) = \frac{(B_K(q)-gI(q))G(q)}{1-C_K(q)}$. We can rewrite $D_{K,g}(q) = \frac{(1-C_K(q))(S(q)-S_{K,g}(q))}{(S(q)-1)S_{K,g}(q)}$. Using the Parseval theorem, we obtain that

$$\bar{J}_{VR}(K,g) = \frac{1}{2\pi}\int_{-\pi}^{\pi}|1-C_K|^2\frac{|S-S_{K,g}|^2}{|S-1|^2|S_{K,g}|^2}|F|^2\Phi_u\,d\omega. \quad (31)$$

Using the $\mathcal{H}_2$-norm of a discrete-time transfer function, it is possible to write $J_{MR}(K,g)$ in (11) as

$$J_{MR}(K,g) = \frac{1}{2\pi}\int_{-\pi}^{\pi}|S-S_{K,g}|^2|W|^2\,d\omega. \qquad (32)$$

Note that (32) is equivalent to (31) if (16) is used. □

Proof of Proposition 3.3 Under Assumption 2, for $\gamma > 0$, it is well known [11] that $\widetilde{A}(\theta) + \widetilde{B}(\theta)J$ is stable and $\|G^*_{K,g,\theta}(q)\|_{\mathcal{H}_2} < \gamma$ if and only if there exists a matrix $P = P^\top \succ 0$ such that

$$\begin{aligned}&P - (\widetilde{A}(\theta) + \widetilde{B}(\theta)J)^\top P(\widetilde{A}(\theta) + \widetilde{B}(\theta)J)\\ &\qquad - (C^* + D^*J)^\top(C^* + D^*J) \succ 0\,, \qquad (33a)\\ &\operatorname{tr}(P) < \gamma^2 = \widetilde{\gamma}\,. \qquad (33b)\end{aligned}$$

By means of the Schur complement and by pre/post-multiplying an invertible matrix, we obtain

$$\begin{bmatrix}Q & \star & \star\\ \widetilde{A}(\theta)Q + \widetilde{B}(\theta)L & Q & \star\\ C^*Q + D^*L & 0 & I\end{bmatrix} \succ 0\,, \qquad (34)$$

where $Q = P^{-1}$ and $L = JQ$. In view of (5) and under Assumption 1, (34) holds for all $\theta \in \Theta$ if and only if (26c) holds for all $i = 1, \ldots, n_v$. Moreover, (33b) is equivalent to (26b) in view of the Schur complement. □

REFERENCES

[1] S. Boyd, L. El Ghaoui, E. Feron, and V. Balakrishnan, *Linear matrix inequalities in system and control theory*. SIAM, 1994.

[2] A. Zecevic and D. D. Siljak, *Control of complex systems: Structural constraints and uncertainty*. Springer Sc. & B. Media, 2010.

[3] M. C. Campi, A. Lecchini, and S. M. Savaresi, "Virtual reference feedback tuning: a direct method for the design of feedback controllers," *Automatica*, vol. 38, no. 8, pp. 1337–1346, 2002.

[4] W. D'Amico and M. Farina, "Virtual reference feedback tuning for linear discrete-time systems with robust stability guarantees based on set membership," *Automatica*, vol. 157, p. 111228, 2023.

[5] M. Massimetti, L. Zaccarian, T. Hu, and A. R. Teel, "Linear discrete-time global and regional anti-windup: an LMI approach," *International Journal of control*, vol. 82, no. 12, pp. 2179–2192, 2009.

[6] S. Tarbouriech and M. Turner, "Anti-windup design: an overview of some recent advances and open problems," *IET control theory & applications*, vol. 3, no. 1, pp. 1–19, 2009.

[7] Z. Duan, J. Zhang, C. Zhang, and E. Mosca, "Robust H_2 and H_∞ filtering for uncertain linear systems," *Automatica*, vol. 42, no. 11, pp. 1919–1926, 2006.

[8] D. Banjerdpongchai and J. How, "Parametric robust H_2 control design using LMI synthesis," in *Guidance, Navigation, and Control Conference*, 1996, p. 3733.

[9] Y.-H. Chang, Y.-Y. Wang, M.-H. Hung, and P.-C. Chen, "Regional stabilizing and H_2 control with actuator saturation using linear matrix inequalities," *Journal of CCIT*, vol. 33, no. 2, pp. 1–13, 2005.

[10] A. Lecchini, M. C. Campi, and S. M. Savaresi, "Virtual reference feedback tuning for two degree of freedom controllers," *Int. J. of Adaptive Contr. and Sig. Proc.*, vol. 16, no. 5, pp. 355–371, 2002.

[11] H. J. van Waarde, M. K. Camlibel, and M. Mesbahi, "From noisy data to feedback controllers: Nonconservative design via a matrix S-lemma," *IEEE Tran. on Aut. Contr.*, vol. 67, no. 1, pp. 162–175, 2020.

[12] M. Campi, A. Lecchini, and S. M. Savaresi, "Virtual reference feedback tuning (VRFT): a new direct approach to the design of feedback controllers," in *Conference on Decision and Control*, vol. 1. IEEE, 2000, pp. 623–629.

[13] F. Bonassi, J. Xie, M. Farina, and R. Scattolini, "An offset-free nonlinear mpc scheme for systems learned by neural narx models," in *Conference on Decision and Control*. IEEE, 2022, pp. 2123–2128.

[14] W. D'Amico, "Data-based control design for linear and recurrent neural network models with stability guarantees. P.hD. thesis," 2024.